Int. J. Heat Mass Transfer. Vol. 29, No. 4, pp. 539–547, 1986
Printed in Great Britain

0017–9310/86 $3.00 + 0.00

Evaporation of water from a partially filled, cylindrical container to a forced convection air flow

A. T. PRATA and E. M. SPARROW
Department of Mechanical Engineering, University of Minnesota, Minneapolis, MN 55455, U.S.A.

(*Received* 12 *July* 1985 *and in final form* 24 *October* 1985)

Abstract—Experiments were performed to investigate the evaporation of liquid water from a partially filled, open-topped cylindrical container situated in the lower wall of a flat, rectangular duct. During the course of the experiments, parametric variations were made of the air flow in the duct (giving rise to a seven-fold variation of the Reynolds number, Re) and of the distance H between the evaporating surface and the top of the container (ranging from 0.1 to 3 container diameters, D). Supplementary experiments were conducted with toluene as the evaporating liquid. It was found that the evaporation rate did not decrease monotonically with increasing H. Rather, a local maximum in the evaporation rate occurred at $H/D \sim 0.5$ for all of the Reynolds numbers investigated. The enhancement of the evaporative mass transfer due to the presence of the maximum ranged from 15 to 35%, depending on the Reynolds number. At all Reynolds numbers except the lowest, vigorous sloshing of the liquid surface occurred at the same H/D at which the evaporation rate displayed a maximum. However, the sloshing is not a prerequisite for the evaporation maximum because such a maximum still occurred when there was no sloshing (i.e. at the lowest Reynolds number). The toluene experiments also indicated the presence of a local maximum in the distribution of the evaporation rate.

INTRODUCTION

THERE is no available information about the evaporation of liquid water from an open-topped, cylindrical container to a forced convection air flow. The air flow passing over the top of the container induces complex, three-dimensional motions both in the evaporating liquid and in the air space above the liquid surface. Owing to the complexity of these motions, it is inappropriate to adapt available knowledge for evaporative mass transfer in simpler situations (e.g. boundary-layer flows). This same complexity virtually precludes a numerical treatment of the problem. It appears, therefore, that experiments are needed to investigate this evaporation situation.

In the present study, measurements were made of the rate of evaporation of water from a partially filled, cylindrical container situated in the lower wall of a flat, rectangular duct. During the course of the experiments, the distance between the evaporating surface and the top of the container (hereafter referred to as the cavity depth) was varied parametrically from about 0.1 to 3 cylinder diameters. The flow rate of the air in the duct was systematically varied over a seven-fold range. Although the main focus of the work was concerned with the evaporation of water, supplementary experiments were performed using toluene (methylbenzene) as the evaporating liquid. The supplementary work was undertaken to confirm an unexpected feature in the observed dependence of the evaporation rate of water on the cavity depth.

A literature survey revealed a general dearth of heat or mass transfer information for open-topped, cylindrical containers in the presence of forced convection flow over the container opening. The only related work is that of Presser [1], who investigated sublimation mass transfer from the cylindrical surface of a container whose base surface did not participate in the mass transfer. Relevant features of the results of ref. [1] will be cited later. Although seemingly unrelated to the present work, the experiments of Wieghardt [2] on the fluid mechanic drag at a plane surface fitted with circular cavities of various depths provide support for the present evaporation rate dependence on cavity depth. For completeness, mention may be made of studies (surveyed in [3]) of the fluid mechanics of cylindrical cavities, with particular emphasis on the organized oscillations induced by the flow passing over the cavity opening.

EXPERIMENTAL APPARATUS AND PROCEDURE

Apparatus

As already noted, the evaporation experiments were performed with a partially filled, cylindrical container situated in the lower wall of a flat, rectangular duct. The description of the apparatus is facilitated by reference to Figs. 1 and 2. The first of these is a schematic, longitudinal sectional view cut through the diameter of the cylindrical container showing both the container and the adjacent portions of the host duct. The second is a top view of the lower wall of the duct illustrating the position of the container opening with respect to the duct width.

As seen in Fig. 1, the cylindrical container was a multi-part assembly of uniform internal diameter D equal to 3.800 cm. The evaporating liquid was confined to the lower portion of the assembly, the mass of which

NOMENCLATURE

A	cross-sectional area of container planform, $\pi D^2/4$
D	diameter of cylindrical container
$\mathscr{D}$	binary mass diffusion coefficient
H	distance between liquid surface and top of container
h	duct height
h	specific enthalpy
K	mass transfer coefficient, equation (1)
L^*	average streamwise dimension of cylindrical container ($= 0.785D$)
p	pressure
Re	Reynolds number, $\rho\bar{u}D/\mu$
Re^*	Reynolds number, $\rho\bar{u}L^*/\mu$
Sh	Sherwood number, $KD/\mathscr{D}$
Sh^*	Sherwood number, $KL^*/\mathscr{D}$
T	temperature
$\bar{u}$	mean velocity of air flow in duct
W	duct width
W	specific humidity.

Greek symbols

μ	viscosity
ρ	density
$\rho_{e,s}$	vapor density of evaporating substance at liquid surface
$\rho_{e,\infty}$	vapor density of evaporating substance in air stream

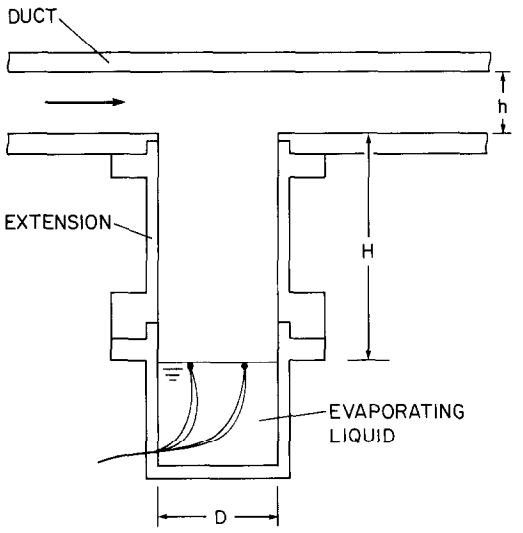

FIG. 1. Longitudinal sectional view cut through the cylindrical container and the adjacent portion of the duct.

(liquid plus container) was designed to accommodate the 200 g capacity of the analytical balance used in the determination of the evaporation rates. The other parts of the asembly are, in effect, extensions which enabled the cavity depth H to be varied over a wide range (H/D from about 0.1 to 3). In practice, as many as three extensions were employed to cover, with overlap, the desired range of H.

The container was made from aluminum rod stock which was carefully machined to the desired dimensions. To prevent electrochemical reactions, the water-containing portion of the assembly was spray-painted and then polished to achieve a thin, protective coating having a smooth surface finish. The interior surfaces of the other parts of the container were also polished for smoothness. Positive sealing between the respective parts of the container and between the container and the duct wall was accomplished by the use of O-rings (not shown). Particular care was taken to ensure that at their mating, the container and the duct wall formed a continuous surface.

The rectangular duct had internal dimensions of 1.928×8.270 cm (height $h \times$ width W), yielding a cross-sectional aspect ratio of 4.29. As seen in Fig. 2, the container opening was centered in the width of the cross section. It should be noted that a substantial clearance ($= 2.235$ cm) was left between the lateral edge of the opening and the adjacent lateral edge of the duct. This clearance ensured that the air flow passing over the opening would be unaffected by spanwise variations in the velocity distribution which necessarily occur adjacent to the duct side walls.

The container opening was located at an axial station situated about 65 duct heights downstream of the inlet cross section of the duct, into which air was drawn from the laboratory room through a sharp-edged inlet. The length of duct between the inlet and the container opening served as a hydrodynamic development section, yielding fully developed flow at the opening. Downstream of the container, the duct continued for a length equal to about 25 heights.

In the main, the duct was fabricated from aluminum plate stock, and its interior surfaces were polished to a high degree of smoothness. The portion of the upper wall of the duct situated directly above the cylindrical container was made of plexiglass to enable the visual observation of the surface of the evaporating liquid.

The system was operated in the open-circuit mode

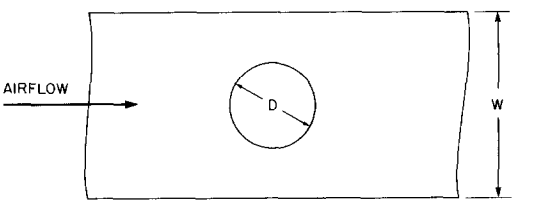

FIG. 2. Top view of the lower wall of the duct illustrating the position of the container opening.

and in suction. The air drawn from the temperature-controlled laboratory passed successively through the rectangular duct, a rectangular-to-circular transition section, a flow meter (a calibrated rotameter), a control valve, and a blower. The blower was situated in a service corridor adjacent to the laboratory, and its compression-heated, vapor-enriched discharge was vented outside the building.

The water used in the experiments was distilled water, and the toluene used in the supplementary experiments was 99.9% pure.

Instrumentation

With regard to instrumentation, mention has already been made of the analytical balance and of the rotameters used for the air flow measurements. The balance had a resolving power of 10^{-4} g, which readily accommodated the evaporation-related change of mass which was typically in the 0.2–0.3 g range. Rotameters of different capacities were used to ensure high accuracy at the various flow rates employed.

As indicated in Fig. 1, two thermocouples were installed in the cylindrical container in order to measure the surface temperature of the evaporating liquid during the experiments. The thermocouples were positioned as close to the surface as was compatible with the evaporation-related recession of the surface. The thermocouples were made from Teflon-coated, 0.0254-cm-diam. chromel–constantan wire chosen for compatibility with water and high e.m.f. per °C. The lead wires were led out of the container through a small aperture in the side wall that was sealed with silicone rubber. Upon emerging from the container, the leads terminated in a subminiature connector which could be readily disconnected from the remainder of the thermocouple circuit. This feature enabled the liquid-filled portion of the container to be completely separated from the apparatus, facilitating its transport to the analytical balance.

Thermocouples were also installed in the duct, both upstream and downstream of the container opening, to measure the air temperature. All thermocouple voltages were read with a multi-channel Hewlett-Packard programmable datalogger having a resolution of 1 μV.

The humidity of the air was measured by a specially designed psychrometric unit. The intake of the psychrometric unit was positioned very close to the entrance of the duct so that the air that was drawn through the unit was a representative sample of the air that passes over the opening of the cavity. The psychrometer consisted of a 76-cm length of 7.6-cm diam. plexiglass tube equipped at its downstream end with a fan which operated in the suction mode. The fan and the tube cross-sectional area were chosen to yield an air flow velocity which provides near-equality of the psychrometric wet-bulb temperature and the thermodynamic wet-bulb temperature. Wet- and dry-bulb thermometers, which could be read to 0.1°F or better, were inserted radially into the tube through cork apertures in the cylindrical wall. The thermometer bulbs were positioned at the tube centerline, with the dry-bulb thermometer upstream of the wet-bulb thermometer (the separation distance was 30 thermometer diameters). Radiation shielding was provided by aluminum foil which completely covered the outside wall of the plexiglass tube.

Procedure

To prepare for a data run, the container was filled with distilled water (or toluene) to a level consistent with the preselected value of H/D. Then, with the container in place in the apparatus, the air flow was initiated. An equilibration period of about one-half hour was allowed, at which time the container was removed from the apparatus and weighed. After the weighing, the thermocouple junctions were positioned just beneath the surface of the liquid, and the container was returned to the duct, thereby initiating the data run.

During the run, the thermocouples were recorded periodically, yielding 10–20 readings per thermocouple, depending on the duration of the run. The air flow rate was carefully monitored and, if necessary, adjusted. Also, during the run, the humidity was measured using the psychrometer. The duration of the run was chosen to limit the evaporation-related recession of the surface. At the termination of the run, the container was removed from the apparatus and weighed.

Supplementary experiments were performed to assess possible extraneous evaporative mass losses during the setup and disassembly of the container, during its transport to and from the balance, and during the weighing. The aggregate of these losses was typically about 0.1% of the evaporation which occurred during the data run proper.

DATA REDUCTION

The average mass transfer coefficient, K, for the evaporation process was obtained from the defining equation

$$K = (\dot{M}/A)/(\rho_{e,s} - \rho_{e,\infty}) \tag{1}$$

where $\dot{M}$ is the rate of evaporation of the liquid from the container during a data run, A is the cross-sectional area of the container planform ($A = \pi D^2/4$), and $\rho_{e,s}$ and $\rho_{e,\infty}$ are the vapor densities of the evaporating substance (subscript e), respectively at the liquid surface and in the air stream in the duct.

The evaporation rate $\dot{M}$ was determined from

$$\dot{M} = \Delta M/\Delta t \tag{2}$$

in which ΔM is the measured change of mass which occurred during the duration of the run Δt. Furthermore, the vapor density $\rho_{e,s}$ was taken to be the gas-phase density of the evaporating substance corresponding to equilibrium with the liquid phase at the surface temperature T_s. For water, $\rho_{e,s}(T_s)$ was obtained from ref. [4], and for toluene from ref. [5]. The

value of T_s was determined by averaging the readings of the two thermocouples used to measure the surface temperature (see Fig. 1). When water was the evaporating substance, the value of $\rho_{e,\infty}$ was obtained from the relative humidity in the air stream, as will be explained shortly; for toluene, $\rho_{e,\infty} = 0$.

To determine the relative humidity in the air stream, some standard thermodynamic relationships are needed. In this connection, h_f and h_g denote the specific enthalpies of saturated liquid water and of saturated water vapor, respectively, while $h_{fg} = h_g - h_f$ denotes the latent heat of evaporation. Furthermore, W_{db} and W_{wb} denote the specific humidities corresponding to the dry-bulb and wet-bulb states, and c_{pa} is the specific heat of dry air. Also, p_{sat} and p_{bar} are, respectively, the saturation pressure of water vapor and the barometric pressure. The molecular weight of water vapor is M_w and of dry air is M_a.

Then, from any standard thermodynamics text (e.g. [6, pp. 396–397]),

$$W_{wb} = (M_w/M_a)p_{sat}(T_{wb})/[p_{bar} - p_{sat}(T_{wb})] \quad (3)$$

and

$$W_{db} = [c_{pa}(T_{wb} - T_{db}) + W_{wb}h_{fg}(T_{wb})]/[h_g(T_{db}) - h_f(T_{wb})] \quad (4)$$

where the temperatures at which the various enthalpies and the saturation pressure are evaluated are indicated in the parentheses; T_{wb} stands for the wet-bulb temperature and T_{db} for the dry-bulb temperature.

With the measured values of the wet-bulb temperature and the barometric pressure, and with a table look-up for p_{sat} at T_{wb}, equation (3) yields W_{wb}. Next, using W_{wb} and with all other quantities on the RHS of equation (4) known from direct measurements or table look-ups, W_{db} is determined.

With the W_{db} value, the partial pressure of the water vapor in the air stream $p_{wv,\infty}$ can be found from

$$W_{db} = (M_w/M_a)p_{wv,\infty}/(p_{bar} - p_{wv,\infty}) \quad (5)$$

from which the relative humidity ϕ follows as

$$\phi = p_{wv,\infty}/p_{sat}(T_{db}). \quad (6)$$

Then, the partial density of water vapor in the air stream is obtained from

$$\rho_{e,\infty} = \rho_{wv,\infty} = \phi\rho_{sat}(T_{db}). \quad (7)$$

Once $\rho_{e,\infty}$ and $\rho_{e,s}$ have been determined, their values, together with $\dot{M}$ from equation (2) and the cross-sectional area A, are substituted into equation (1) to yield the mass transfer coefficient, K. All of the thermodynamic properties needed in the foregoing calculations were taken from ref. [4], except for c_{pa} from ref. [7].

The mass transfer coefficient K was recast in dimensionless form in terms of the Sherwood number

$$Sh = KD/\mathscr{D} \quad (8)$$

where $\mathscr{D}$ is the binary mass diffusion coefficient. For the water, $\mathscr{D}$ was evaluated from an empirical expression given in [8, p. 10], whereas, for toluene, $\mathscr{D}$ was obtained from the well-established form [9]

$$\mathscr{D} = CT^{1.75}/p. \quad (9)$$

The constant C for the toluene–air system was evaluated from the data of ref. [10], yielding the working equation

$$\mathscr{D} = 0.402T^{1.75}/p \quad (10)$$

where $\mathscr{D}$ is in $cm^2\ s^{-1}$, T is in K, and p is in Pa.

Two quantities were used to parameterize the Sherwood number results, the Reynolds number Re and the dimensionless distance H/D between the surface of the evaporating liquid and the top of the container. The Reynolds number was defined as

$$Re = \rho\bar{u}D/\mu \quad (11)$$

where ρ and $\bar{u}$ are, respectively, the density and mean velocity of the duct flow (taking the moisture into account). The viscosity μ was taken to be that of dry air [11] since the presence of water vapor was estimated to cause departures of no more than 0.2% [12].

The distance H between the liquid surface and the top of the container was determined indirectly. First, the mass of the liquid in the container was found by subtracting the known mass of the empty container from that measured with the liquid in place. Then, from the knowledge of the liquid density (water [13], toluene [5]) and the cross-sectional area of the container planform, the height of the liquid in the container was calculated. This height was subtracted from the overall distance between the bottom and the top of the container, yielding H (see Fig. 1) and, consequently, H/D. As will be elaborated in the discussion of the results, the liquid surface is not always flat. Therefore, H represents a *mean* distance between the actual liquid surface and the top of the container.

RESULTS AND DISCUSSION

Mass transfer coefficients

The mass transfer coefficients for evaporation of water are presented in dimensionless form in Fig. 3, where the Sherwood number Sh is plotted as a function of the dimensionless distance H/D between the evaporating surface and the top of the container, which was varied from 0.1 to 3. Results are shown for four parametric values of the Reynolds number ranging from 7300 to 48 600.

An overall examination of the figure reveals an unexpected dependence of the evaporation rate on the distance H that separates the liquid surface from the container opening. In particular, instead of a monotonic decrease, the variation of the evaporation rate with increasing distance displays a local maximum. The maximum occurs between $H/D = 0.4$ and 0.5,

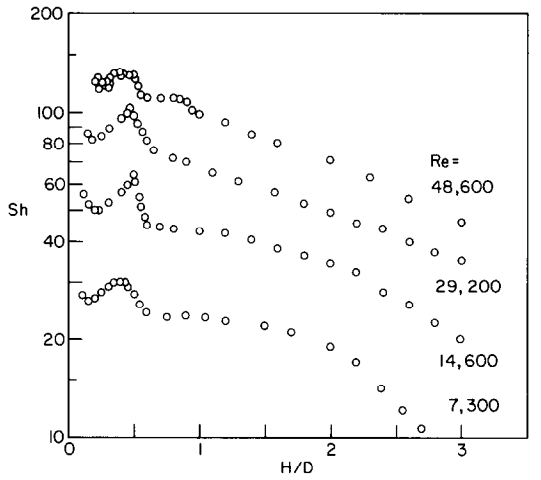

FIG. 3. Evaporation results for water.

without a systematic dependence on the Reynolds number. For $Re = 7300$, the maximum is more rounded than are those for $Re = 14\,600$ and 29 200. At $Re = 48\,600$, the maximum is not as well defined as it is for the other Reynolds numbers.

The extent of the mass transfer enhancement at the maximum was estimated by comparing the measured Sherwood number with that obtained by fairing a curve through the Sh vs H/D distribution while ignoring the presence of the maximum. For $Re = 7300$, 14 600, 29 200 and 48 600, the enhancements were, respectively, about 20, 35, 30, and 15%.

The other features of the Sh vs H/D distributions will now be described. Starting with $H/D \sim 0.1$, the smallest H/D at which accurate mass transfer measurements could be made, there is an indication of a decrease of Sh with H/D, which is arrested by the attainment of a local minimum at $H/D \sim 0.2$. Then, as H/D increases further, the aforementioned Sherwood number maximum occurs. The relatively steep downslope which follows the maximum gives way to a much more gradual dropoff which, for certain Reynolds numbers, has a plateau-like character. Still further increases in H/D give rise to progressively smaller Sh values and, at the lower Reynolds numbers, a rapid dropoff sets in at larger H/D.

It is believed that the results presented in Fig. 3 are valid for duct geometries other than that employed in the present experiments. This broadened validity requires that the air flow in the duct which arrives at the site of the container be fully developed and that there be a substantial lateral clearance between the container opening and the duct sidewalls (to eliminate duct end effects). The influence of the duct height on the Sherwood number was addressed in ref. [14] for the case of naphthalene sublimation. It was found there that for a given Re and H/D, Sh was independent of the duct height. The correlation of the results of Fig. 3 will be dealt with later, after physical insights about the flow pattern in the container are conveyed.

Configurations of the liquid surface

The presence of the aforementioned mass transfer maxima prompted a careful examination of the surface of the evaporating liquid. At the lowest Reynolds number, the surface was quiescent for all H/D, even for the smallest values investigated. As Re increased, small ripples started to appear on the liquid surface. For small H/D, the ripples were stronger than those at large H/D. In fact, if H/D were continuously increased, the ripples eventually disappeared, and the liquid surface became quiescent. Also, for a fixed H/D, larger Reynolds numbers gave rise to more ripples on the liquid surface.

A sloshing of the liquid occurred at $H/D \sim 0.4$–0.5 for Reynolds numbers other than 7300 (the liquid surface was always flat at this value of Re). As H/D approached the value corresponding to the maximum Sherwood number, the liquid started to slosh. The amplitude of the sloshing motion increased and attained its largest value at the H/D at which Sh was a maximum. Further increases of H/D caused the amplitude to decrease and, eventually, the sloshing motion died away.

The form of the oscillation can be described with the aid of Fig. 4. This figure is a plan view of the cylindrical container showing + and − signs which indicate the level of the liquid relative to that in the absence of sloshing (flat surface). The + signs correspond to the high points of the liquid surface at a particular instant of time, while the − signs depict the low points of the surface at the same instant. Owing to the sloshing motion, there is a periodic reversal of the elevation and depression of the surface. For example, if τ is the period of the sloshing, the configuration of the surface for the first half of τ is that shown in Fig. 4(a), while for the second half, the configuration is that depicted in Fig. 4(b).

Also shown in Figs. 4(a) and (b) are a pair of straight lines. The sloshing motions roll back and forth along each line as time passes, causing the aforementioned reversal of high and low points. The neighborhood of the intersection of the lines (i.e. at the center of the circular planform) is relatively quiescent. In general, owing to the interaction of the sloshing motions which roll along the two lines, the shape of the surface is highly complex.

The frequency of the sloshing was visually estimated to be 4–5 Hz at $Re \sim 48\,600$. This frequency could not be accurately determined because of the complexity of the motion. The amplitude of the sloshing was highly

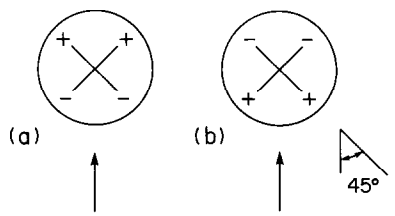

FIG. 4. Schematic top view of the cylindrical container showing the pattern of sloshing of the water surface.

dependent on the Reynolds number. For $Re = 14\,600$, the sloshing was barely observable, but for $Re = 48\,600$ and at a nominal $H/D \sim 0.5$, the liquid reached the rim of the container, which corresponded to a height of 2 cm above the nominal liquid level.

Although the most vigorous sloshing and the maximum evaporation rate occurred at the same H/D, sloshing is not a prerequisite for the evaporation maximum since such a maximum was still observed when the surface was quiescent, i.e. at $Re = 7300$. Both the sloshing and the evaporation maximum are believed to be caused by unsteady motions of the air in the container above the liquid surface. At low Reynolds numbers, the stresses associated with these motions are too small to induce observable movement of the liquid.

In addition to the vigorous sloshing at the highest Reynolds number, a definite fore-to-aft downward tilt of the liquid surface was observed. The tilt occurs because the air flow entering the container impinges on the downstream portion of the liquid surface and depresses the liquid in that region.

Correlation of the mass transfer results

The nature of the mass transfer results at the highest Reynolds number (e.g. the smeared nature of the maximum) reflects the hyper-vigorous hydrodynamics that have just been discussed. In this light, it would not be expected that the results for this Reynolds number would correlate with those for the others. At the lowest Reynolds number, $Re = 7300$, the corresponding ductflow Reynolds number of 6000 (based on the duct hydraulic diameter) is indicative of the transition regime. For this Reynolds number, the motions of the air within the container were too feeble to perturb the water surface. Consequently, it is unlikely that the Sherwood numbers for this case would correlate with those for higher Reynolds numbers (note the rounding of the maximum for $Re = 7300$ and its shift toward smaller H/D). The foregoing discussion suggests that the intermediate Reynolds numbers hold the greatest promise for the correlation of the mass transfer results.

A correlation effort was, in fact, attempted for all the Reynolds numbers and, in accordance with the foregoing expectations, a satisfactory correlation was achieved only for the intermediate values. Furthermore, the correlation was successful only in the range of smaller H/D which, fortunately, encompasses the highest evaporation rates and is, therefore, of primary interest from the standpoint of practice.

Figure 5 shows the correlation of the Sherwood number results for $Re = 14\,600$ and 29 200. As seen there, the data for the two Reynolds numbers are brought together by employing the group $Sh/Re^{0.75}$, which indicates that $Sh \sim Re^{0.75}$ for the operating conditions depicted in the figure. It is believed that the correlation conveyed by Fig. 5 should be valid for Re as low as 10 000 (duct Reynolds number of about 8000), which marks the lower limit of fully turbulent flow in the duct. In addition, an extension of the correlation to $Re \sim 35\,000$ appears warranted.

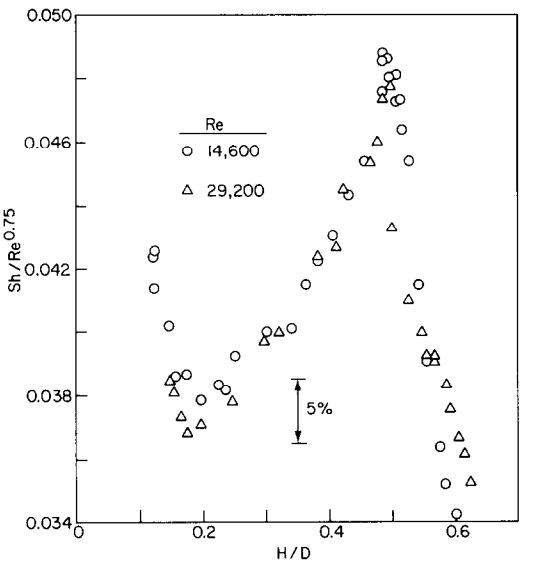

FIG. 5. Correlation of the Sherwood number results for water for $Re = 14\,600$ and 29 200.

Elaboration of the mass transfer maxima

The presence of the unexpected maximum in the distribution of Sh vs H/D prompted both further experiments and a careful survey of the literature to identify related situations where similar maxima have been encountered. In considering the supplementary experiments, a liquid having thermophysical properties different from those of water was sought. In this regard, toluene was found to be suitable, and it was additionally attractive because it is readily available in a highly pure form and because its properties are very well established. Toluene is highly volatile and has an evaporation rate that is much higher than that of water. The Schmidt number of toluene is 1.83, compared with the Schmidt number of 0.60 for water.

In Fig. 6, the Sherwood number results for the evaporation of toluene are compared with those for the evaporation of water at a common Reynolds number of

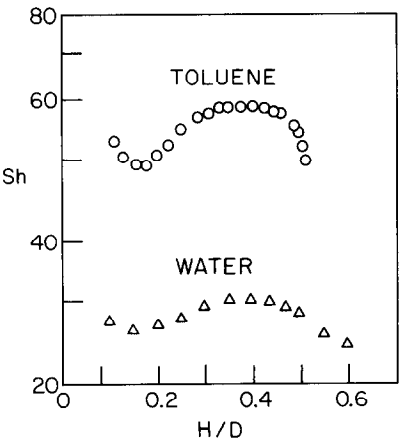

FIG. 6. Comparison of Sherwood number results for toluene and water, $Re = 7300$.

7300. As seen there, the variation of the Sherwood number with H/D has the same shape for the two evaporating liquids. In particular, the toluene results also display a local maximum, thereby indicating that the presence of the maximum is not restricted to the properties of a specific evaporating substance.

Turning now to the literature, attention may be directed to the work of Presser [1], who investigated the sublimation of naphthalene from the cylindrical surface of an open-topped cavity whose base did not participate in the mass transfer process. The cavity was situated in the lower wall of a rectangular duct in a setup similar to the present experimental arrangement. For turbulent air flow in the duct, the results of ref. [1] suggested the presence of a local maximum in the distribution of the mass transfer rate as a function of the cavity depth. However, the presentation variables used there did not provide direct evidence of the maximum (indeed, in a correlation of the results, the maximum was actually suppressed). To explore this issue, the results of ref. [1] were rephrased and replotted as shown in Fig. 7. On the ordinate, the Sherwood number Sh^* is defined as $KL^*/\mathscr{D}$, where L^* is the average streamwise dimension of the cavity opening ($= 0.785D$). The mass transfer coefficient, K, is that defined in equation (1), where $\dot{M}$ is now the sublimation rate of naphthalene and, as before, A is equal to $\pi D^2/4$. Therefore, with these definitions, Sh^* is a dimensionless mass transfer rate. The Reynolds number Re^* is equal to $\rho \bar{u} L^*/\mu$.

From the figure, it is seen that the mass transfer distribution clearly displays a local maximum and that the maximum occurs at $H/D \sim 0.5$. Also of interest is the local minimum at $H/D \sim 0.15$, which is reminiscent of a corresponding minimum in the present Sh distributions. Note that following the post-maximum downslope of the Sh^* distribution in Fig. 7, the mass transfer rate increases monotonically with H/D. This occurs because the area of the subliming surface increases as H/D increases.

Another manifestation of the fluid flow processes which cause the mass transfer maxima observed here was encountered in studies by Wieghardt [2] of the drag on a flat plate. In the presence of cylindrical cavities in the plate, the incremental drag relative to that for a smooth plate attained a maximum value at $H/D \sim 0.5$.

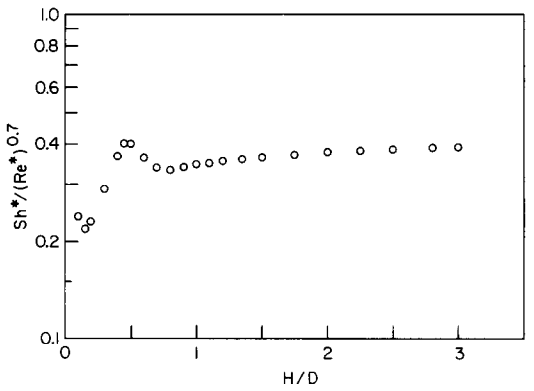

FIG. 7. Sherwood number results from ref. [1] for sublimation of naphthalene from the cylindrical surface of a cavity.

In a thesis [14] which was motivated by the present work, experiments were performed with a cylindrical cavity whose base was a naphthalene disk. The cylindrical wall of the cavity did not participate in the mass transfer process. The cavity was situated in the lower wall of a rectangular duct, as in the present investigation. In the results of ref. [14], for all of the Reynolds numbers investigated (ranging from 8800 to 88 400), a well-defined maximum was also observed in the distributions of Sh vs H/D. Furthermore, for all Reynolds numbers for which the duct flow was fully turbulent, the maximum occurred at $H/D \sim 0.5$. At lower Reynolds numbers, the maximum tended to recede toward lower H/D values.

CONCLUDING REMARKS

Forced convection evaporation from a partially filled, open-topped cylindrical container was investigated experimentally. The container was situated in the lower wall of a flat, rectangular duct such that the opening of the container was flush with the surface of the wall. The primary experiments were conducted with water as the evaporating liquid, and toluene was used in supplementary experiments.

During the course of the experiments, the velocity of the air flow passing through the duct was varied parametrically, yielding a seven-fold variation of the Reynolds number. Also varied was the distance, H, between the evaporating surface and the top of the container, ranging from 0.1 to 3 times the cylinder diameter D. The evaporation results were presented in dimensionless form in terms of the Sherwood number, Sh, which was plotted as a function of H/D for parametric values of the Reynolds number. The quantitative measurements of the evaporation mass transfer were supplemented by careful visual observations of the surface of the liquid.

The Sherwood number did not display a monotonic decrease as the distance between the liquid surface and the top of the container increased. Rather, a local maximum in the Sh vs H/D distribution occurred at $H/D \sim 0.5$ for all of the investigated Reynolds numbers. The enhancement of the mass transfer due to the presence of the maximum ranged from 15 to 35%, depending on the Reynolds number. At H/D values greater than that at the maximum, the Sherwood number decreased with increasing H/D. The Sherwood number results were correlated at intermediate Reynolds numbers by a relation of the form $Sh/Re^{0.75} = f(H/D)$.

The supplementary experiments performed with toluene also indicated the presence of a local maximum in the Sh vs H/D distribution.

Sloshing occurred at all Reynolds numbers other than the lowest value investigated. The sloshing was most vigorous at $H/D \sim 0.5$, the same H/D at which the

evaporation rate displayed a maximum. It is believed that the sloshing is not a prerequisite for the evaporation maximum, since such a maximum still occurred when the surface was quiescent, i.e. at the lowest Reynolds number.

Acknowledgement—Support accorded to A. T. Prata by Universidade Federal de Santa Catarina and Conselho Nacional de Desenvolvimento Científico e Tecnológico (CNPq) of Brazil is gratefully acknowledged.

REFERENCES

1. K. H. Presser, Empirische gleichungen zur berechnung der stoff- und warmeubertragung fur den spezialfall der abgerissenen stromung, *Int. J. Heat Mass Transfer* **15,** 2447–2471 (1972).
2. H. Schlichting, *Boundary Layer Theory*, 7th edn, pp. 655–656. McGraw-Hill, New York (1979).
3. D. Rockwell and E. Naudascher, Review—Self-sustaining oscillations of flow past cavities, *J. Fluids Engng* **100,** 152–165 (1978).
4. J. H. Keenan, F. G. Keyes, P. G. Hill and J. G. Moore, *Steam Tables*. Wiley, New York (1969).
5. C. L. Yaws, *Physical Properties: A Guide to the Physical, Thermodynamic and Transport Property Data of Industrially Important Chemical Compounds*. McGraw-Hill, New York (1977).
6. W. C. Reynolds and H. C. Perkins, *Engineering Thermodynamics*, 2nd edn. McGraw-Hill, New York (1977).
7. Y. S. Touloukian and T. Makita, *Thermophysical Properties of Matter, Specific Heat*, Vol. 6. IFI/Plenum, New York (1970).
8. T. K. Sherwood and R. L. Pigford, *Absorption and Extraction*, 2nd edn. McGraw-Hill, New York (1952).
9. R. C. Reid, J. M. Prausnitz and T. K. Sherwood, *The Properties of Gases and Liquids*, 3rd edn. McGraw-Hill, New York (1977).
10. G. A. Lugg, Diffusion coefficients of some organic and other vapors in air, *Analyt. Chem.* **40,** 1072–1077 (1968).
11. Y. S. Touloukian and T. Makita, *Thermophysical Properties of Matter, Viscosity*, Vol. 11. IFI/Plenum, New York (1970).
12. E. A. Mason and L. Monchick, Survey of equations of state and transport properties of moist gases. In *Humidity and Moisture* (edited by A. Wexler), Vol. 3, pp. 257–272. Reinhold, New York (1965).
13. G. S. Kell, Precise representation of volume properties of water at one atmosphere, *J. chem. Engng Data* **12,** 66–69 (1967).
14. D. L. Misterek, Heat and mass transfer from the bottom surface of a recessed cavity. M. S. thesis, Department of Mechanical Engineering, University of Minnesota, Minneapolis, MN (1985).

EVAPORATION D'EAU DANS UN RESERVOIR CYLINDRIQUE, PARTIELLEMENT REMPLI, PAR UNE CONVECTION FORCEE D'AIR

Résumé—On étudie l'évaporation d'eau liquide d'un réservoir cylindrique, ouvert au sommet, situé dans la paroi inférieure d'un conduit rectangulaire plat. Pendant les expériences, on assure les variations paramétriques du débit d'air dans le conduit (jusqu'à sept fois le nombre de Reynolds, *Re*) et la distance H entre la surface libre et le sommet du réservoir). D'autres expériences sont faites avec du toluène. On trouve que la vitesse d'évaporation ne décroît pas de façon monotone quand H augmente. Il existe un maximum à $H/D \sim 0{,}5$ pour tous les nombres de Reynolds étudiés. L'accroissement du transfert thermique dû au maximum est entre 15 et 35%, selon le nombre de Reynolds. A tous les nombres de Reynolds sauf le plus faible, une vigoureuse agitation de la surface libre apparait pour le même H/D où se produit le maximum d'évaporation. Mais ceci n'est pas lié au maximum car celui-ci apparait sans agitation (au faibles nombres de Reynolds). Le toluène montre la présence d'un maximum local dans la distribution de la vitesse d'évaporation.

VERDUNSTUNG VON WASSER AUS EINEM TEILWEISE GEFÜLLTEN ZYLINDRISCHEN BEHÄLTER IN EINE ERZWUNGENE LUFTSTRÖMUNG

Zusammenfassung—Die Verdunstung von flüssigem Wasser aus einem teilweise gefüllten zylindrischen Behälter, welcher sich an der unteren Wand eines flachen rechteckigen Kanals befindet und nach oben offen ist, wurde experimentell untersucht. Bei den Versuchen wurde der Luftstrom im Kanal (bis zur siebenfachen Reynoldszahl, *Re*) und der Abstand H zwischen der Verdunstungsoberfläche und dem oberen Rand des Behälters ($0, 1 < H/D < 3$) variiert. Mit Toluol als verdunstendem Fluid wurden zusätzliche Experimente durchgeführt. Es ergab sich, daß die Verdunstungsrate mit steigenden Werten von H nicht monoton abfällt, es ergibt sich ein lokales Maximum der Verdunstungsrate bei $H/D \approx 0{,}5$ für alle Reynoldszahlen. Die Erhöhung der Verdaunstungsrate lag bei 15 bis 35%, abhängig von der Reynoldszahl. Bei allen Reynoldszahlen, ausgenommen der kleinsten, zeigte sich eine starke Wellenbildung an der Flüssigkeitsoberfläche und zwar gerade bei den Werten von H/D, bei welchen die Verdunstungsrate das Maximum zeigte. Jedoch ist die Wellenbildung keine Voraussetzung für das Verdunstungsmaximum, weil ein solches Maximum auch dann auftrat, wenn keine Wellenbildung vorhanden war (d.h. bei der kleinsten Reynoldszahl). Die Toluol-experimente zeigten ebenso ein lokales Maximum bei der Verdunstungsrate.

ИСПАРЕНИЕ ВОДЫ ИЗ ЧАСТИЧНО ЗАПОЛНЕННОЙ ЦИЛИНДРИЧЕСКОЙ ЕМКОСТИ В ВЫНУЖДЕННО-КОНВЕКТИВНЫЙ ВОЗДУШНЫЙ ПОТОК

Аннотация—Экспериментально изучено испарение воды из частично заполненной открытой сверху цилиндрической емкости, которая сообщается с каналом прямоугольного сечения. В экспериментах варьировали параметры потока воздуха в канале (семикратное изменение числа Рейнольдса *Re*) и расстояния H между поверхностью испарения и верхней частью емкости (изменяющегося в диапазоне от 0,1 до 3 диаметров емкости *D*). Проведены также эксперименты с толуолом вместо воды. Найдено, что с увеличением H скорость испарения падает немонотонно. Локальный максимум скорости испарения достигается при *H*/*D* 0,5 для всех исследованных чисел Рейнольдса. Максимальное увеличение скорости испарения составляло от 15 до 35% в зависимости от числа Рейнольдса. При всех числах Рейнольдса за исключением наименьших происходит сильное возмущение поверхности жидкости при тех же значениях *H*/*D*, при которых скорость испарения имеет максимум. Однако это возмущение не является необходимым условием существования максимума испарения, поскольку он существует и тогда, когда возмущение отсутствует (т.е. при наименьших числах Рейнольдса). В экспериментах с толуолом имеется локальный максимум скорости испарения.